A Unified View of Diffusion Maps and Signal Processing on Graphs

Ayelet Heimowitz and Yonina C. Eldar

Abstract—In this paper we explore the connection between diffusion maps and signal processing on graphs. We aim to create a common ground for both approaches through the definition of the graph shift operator as the transition matrix of a Markov chain defined on the graph. We then demonstrate several advantages of this definition, as well as the resulting diffusion map interpretation of operations defined in signal processing on graphs. For example, one advantage is the ability to process a graph signal over a Euclidean domain. Another advantage is the ability to use the Nyström extension for computationally efficient interpolation of signals over a graph. In addition, we present a definition of signals over a graph and show the relation between the diffusion embedding vectors and the spectrum of these signals.

I. INTRODUCTION

Recent years have seen a huge increase in available data from sources such as social networks, government agencies, commercial and academic bodies and more. Such data sets can include, for example, blogs, temperature measurements and information on customer preferences. Graphs are a popular model for the underlying geometry of data. Each data element (point) is represented as a node, and the pairwise connections between the different points are modeled as edges. Using this methodology, any data set can be modeled as a graph, so long as the data points are represented as a vector of features in \mathbb{R}^M , M>0, and some similarity measure between data points is defined.

As an example, consider a data set of images of written digits, *e.g.* the MNIST data set [1]. Each data point is an image of a digit, and is represented as a node. The similarity between two points (*i.e.* two images of digits) is expressed through the edge weights. In the context of social networks, each user is a node in the graph, and the relationships between users are modeled as edge weights [2]. Such relationships may be for example friendship or collaboration.

The author Ayelet Heimowitz is with the Program in Applied and Computational Mathematics, Princeton University, Princeton, NJ. The author Yonina C. Eldar is with the Andrew and Erna Viterbi Faculty of Electrical Engineering, Technion - Israel Institute of Technology, Haifa, Israel, e-mail: ayeltg@gmail.com, yonina@ee.technion.ac.il;

This project has received funding from the European Union's Horizon 2020 research and innovation program under grant agreement No. 646804-ERC- COG-BNYQ.

This research was carried out while the first author was a post-doctoral researcher at the Department of Electrical Engineering, Technion, Haifa, Israel.

Graphs can be divided into several categories. The first is weighted graphs versus non-weighted graphs. A weighted graph is employed when the strength of a connection between two data points is important. The edge weights encode the strength of this connection and are often restricted to be nonnegative. Non-weighted graphs are used when the mere existence of a connection is sufficient pairwise information. For example, a data set of academic papers, where the connections are citations, may be described by a non-weighted graph, as any paper either cites another paper or does not.

A second category for graphs is directed graphs versus undirected graphs. In a directed graph the pairwise relationship between points is a-symmetric. In this case each edge must have a specified node of origin and a specified target node. In an undirected graph the pairwise relationship between nodes is symmetric, and thus the edges are bidirectional. Returning to the example of the data set of academic papers, a paper may cite a relevant paper with an earlier publishing date, however, no paper can cite a later paper. Thus, it makes sense that the pairwise relationship should be a-symmetric. On the other hand, assuming paper A cites paper B, we may conclude that both papers have relevance to each other, and model the pairwise relationship as symmetric. The model should depend both on the data and on the application.

In recent years the community of signal processing has shifted its attention to graph signals, which are signals residing over irregular domains represented as weighted graphs [3], [4], [5], [6], [7]. A graph signal can reside over domains represented as weighted and undirected graphs with non-negative weights [3], which allows to build upon results in spectral graph theory [8]. The graph signal may alternatively be defined over domains represented as general graphs, which are not restricted to be undirected or to have non-negative weights [4]. This approach relies on algebraic signal processing theory.

In previous literature, the graph signal was defined as a mapping of each node in a graph to a scalar [4], [5], [6], [9]. The graph signal was then represented as a vector in \mathbb{R}^N . In this paper we modify this definition and define the graph signal to be a mapping of each node to some scalar (real or complex) such that the geometry of the graph is adhered to. A vector (signal) that obeys the graph geometry is smooth over the edges of the graph. This smoothness is determined through a measure which assigns a numerical value detailing the change of the signal over the graph edges. Smoothness criteria have been discussed, for example, in [7], [10]. Here we suggest the Markov variation, which is a probabilistic smoothness measure for graph signals which relies on the relationship between the

graph signal and the diffusion maps framework of Coifman and Lafon [11].

The diffusion map framework was suggested with the goal of providing a better understanding of the underlying irregular domain represented as a weighted undirected graph. It does this through a geometry preserving embedding of the nodes of the graph, wherein each node of the graph is represented as a vector in a Euclidean space and the distances between the vectors correspond to the connectivity between the nodes they represent. As this embedding preserves the local geometry of the graph, and since the graph signal is related to the geometry of the graph, there exists a connection between the diffusion embedding vectors and the graph signal. In order for a vector to be a graph signal, it must map any two nodes with close (in the ℓ_2 sense) diffusion embedding vectors to similar values.

In this paper we make use of the connection between the diffusion map embedding and the graph signal. First, we propose a definition of graph signals which explicitly takes the graph geometry into account through the diffusion map embedding. This definition restricts the domain of graph signals from \mathbb{R}^N to a class of signals that is limited by the geometry of the graph and formalizes the connection between the irregular domain represented by a graph and the graph signal. Second, we present several advantages to using the diffusion embedding vectors of a weighted undirected graph for operations defined in the field of signal processing on graphs.

In particular, one advantage we demonstrate is that a function on a node of the graph is equivalent to a function on the embedding, allowing to process the graph signal in a Euclidean space where ℓ_2 distances preserve the local geometry of the graph. This means that signal processing on a graph can be performed in practice over vectors in a Euclidean space instead of nodes and edges of a graph. An example application of this approach is graph signal interpolation. In this problem, the graph signal over a subset of nodes A is given, and the goal is to estimate the signal over the remaining nodes. We show that this problem can be solved over vectors in a Euclidean space rather than nodes of a graph. Another benefit is the use of the Markov matrix in the diffusion maps framework. We demonstrate this advantage through a computationally efficient method for graph signal interpolation using a variation on the Nyström extension.

This paper is organized as follows. Section II contains background for the diffusion maps framework and signal processing on graphs. In Section III we introduce our definition of signals defined on graphs. Section IV discusses the connection between the diffusion maps framework and signal processing on graphs. In Section V we consider several advantages of incorporating the diffusion map embedding into signal processing on graphs. Experimental results demonstrating our proposed graph interpolation method are presented in Section VI.

II. GRAPHS AND DIFFUSION MAPS

A. From Data Sets to Graphs

A graph is denoted as $\mathcal{G} = \langle \mathcal{V}, \mathcal{E} \rangle$ where \mathcal{V} is the set of nodes and \mathcal{E} is the set of edges. For weighted graphs we denote the affinity matrix containing edge weights as \mathbf{W} . The ijth element of the affinity matrix specifies the weight of an edge between node v_i and node v_j . If no edge exists between these nodes, then $W_{i,j}$ is set to 0.

A graph can be either directed or undirected. The edges of a directed graph each have a node of origin and a target node. An edge between nodes v_i and v_j in a directed graph is denoted as $(v_i, v_j) \in \mathcal{E}$. The edges in an undirected graph are bidirectional. This necessitates the affinity matrix of any undirected graph to be symmetric. An edge between node v_i and node v_j in an undirected graph is denoted as $\{v_i, v_j\} \in \mathcal{E}$.

The diffusion maps framework [11] deals with weighted undirected graphs with non-negative weights. Such a graph is a representation of some data set $\mathcal{X} = \{x_1, \dots, x_N\}$ containing N data elements (points). Each node of the graph represents a data element. The weights of the edges are determined through an (application dependent) symmetric and non-negative kernel function $k: \mathcal{X} \times \mathcal{X} \to \mathbb{R}$. The affinity matrix \mathbf{W} is built such that $W_{i,j} = k$ (x_i, x_j) . The symmetry property of the kernel function limplies that

$$W_{i,j} = k(x_i, x_j) = k(x_j, x_i) = W_{j,i},$$

and the non-negativity property leads to

$$W_{i,j} = k\left(x_i, x_j\right) \ge 0.$$

For an example of an application dependent kernel we consider a data set of temperature measurements taken once a day (over an extended period of time) by 150 sensors placed in known locations around the US [4]. This data set has 150 data elements, corresponding to 150 sensors. A graph representing this set will have 150 nodes, where each node v_i corresponds to a single sensor x_i . If the temperature measured at sensor x_i is an indication of the temperature we expect to measure at sensor x_j then we would like the nodes corresponding to these sensors to be connected by an edge, i.e., $\{v_i, v_i\} \in \mathcal{E}$. It is a fair assumption that temperatures measured by sensors in close proximity to each other are similar. However, the temperature measured by distant sensors are neither necessarily similar nor necessarily different. Therefore, we only want sensors located in geographical proximity to be connected by an edge. In this case a Gaussian kernel may be a good choice to determine the weight of each edge.

Once the kernel is selected, and the symmetric affinity matrix has been computed, the diffusion maps framework computes the spectral properties of the resulting Markov matrix. The Markov matrix defined on \mathcal{G} is a normalization of the affinity matrix such that each row of the Markov matrix sums to 1. Specifically, the Markov matrix is given by

$$\mathbf{P} = \mathbf{D}^{-1}\mathbf{W},\tag{1}$$

where \mathbf{D} is the diagonal matrix that contains in its *ii*th element the degree of node v_i ,

$$D_{i,i} = d(v_i) = \sum_{j=1}^{N} W_{i,j}.$$

The elements of \mathbf{P} can be interpreted as transition probabilities encoding the pairwise relationships between nodes in the graph (as they are proportional to the elements of \mathbf{W}). Consider the matrix \mathbf{P}^t . The ijth entry of \mathbf{P}^t contains the transition probabilities from v_i to v_j in t time steps, or, in other words, taking into account the transition probabilities of all length t paths originating at v_i and concluding at v_j . Similar to \mathbf{P} , the matrix \mathbf{P}^t also encodes the relationship between pairs of data elements, this time at a higher scale (considering paths and not just immediate neighbors). The ijth entry of matrix \mathbf{P}^t is high if and only if there is a high probability of transition between node v_i and v_j in t steps.

Figure 1 demonstrates the pairwise transition probabilities in the MNIST data set for several scales. From the 60000 training images contained in the MNIST data set, we randomly select 500 images of each digit and construct a graph $\mathcal{G} = \langle \mathcal{V}, \mathcal{E} \rangle$ to represent the reduced data set of 5000 selected images of handwritten digits. Digit i is represented by nodes $\{v_{500i+1}, \dots, v_{500(i+1)}\}$. We choose a suitable kernel k with the goals of differentiating between different digits while keeping the number of edges small. This kernel can be, for example, a Gaussian kernel with a relatively small bandwidth. The Markov matrix and powers of the Markov matrix for this example are depicted in Fig. 1. It is clear from Fig. 1 that there is a high probability of transition in $t=2,\ldots,12$ steps between nodes that represent images of the same digit and a low probability of transition between nodes that represent images of different digits. In other words, powers t = 2, ..., 12 of the Markov matrix reflect the clusters of the data set. For large values of t, such as t = 1024, the probability to transition to any node in t steps does not depend on the node of origin.

The Markov matrix P will be used extensively throughout the paper. In the lemma and proposition below we summarize some of its key properties.

Lemma 1. The Markov matrix is diagonalizable.

Proof. See the appendix.

Since $\mathbf{P} \in \mathbb{R}^{N \times N}$ is diagonalizable, it has N eigenvalues and N eigenvectors. In the proposition below we denote the eigenvectors and eigenvalues of \mathbf{P} as $\{\psi_i\}_{i=1}^N$ and $\{\lambda_i\}_{i=1}^N$, respectively. We further denote the eigenvectors and eigenvalues of the normalized graph Laplacian, defined by

$$\mathbf{L} = \mathbf{D}^{-\frac{1}{2}} \left(\mathbf{D} - \mathbf{W} \right) \mathbf{D}^{-\frac{1}{2}}, \tag{2}$$

as $\{\mathbf{u}_i\}_{i=1}^N$ and $\{\tilde{\lambda}_i\}_{i=1}^N$.

Proposition 1. The eigenvectors and eigenvalues of the Markov matrix obey the following:

1)
$$\psi_i = \mathbf{D}^{-\frac{1}{2}} \mathbf{u}_i$$
, $\lambda_i = 1 - \tilde{\lambda}_i$.

 $|\lambda_i| \leq 1$

3) The leading eigenvector of the Markov matrix is constant.

Proof. The proof of parts 1 and 2 are given in the appendix. To prove part 3, we note that each row in the Markov matrix sums to 1. Thus,

$$\mathbf{P1} = 1 \cdot \mathbf{1},\tag{3}$$

where 1 is the all ones vector. We see that 1 is an eigenvalue of \mathbf{P} , and is associated with a constant eigenvector. We know from part 2 of the proposition that the eigenvalues are upper bounded by 1. Therefore, the constant eigenvector must be the leading one.

Another observed property of the Markov matrix is that the eigenvalues decrease to 0 for many graphs that represent real life data sets [11]. In Section II-B we show that this is the basis of the dimension reduction property of diffusion maps [11], [12], [13].

B. Diffusion Maps

Coifman and Lafon [11] presented a diffusion map representation for each node of a weighted undirected graph (each element of a data set) as a vector of up to N-1 coordinates. Thus, the data set is first represented as a graph, and the graph is then embedded into a Euclidean space.

The embedding defined by Coifman and Lafon is based on the spectral properties of the Markov matrix. Denote the set of eigenvectors of \mathbf{P} as $\{\psi_i\}_{i=1}^N$, with corresponding eigenvalues $\{\lambda_i\}_{i=1}^N$. A family of *diffusion maps* $\{\Psi_t\}_{t\in\mathbb{N}}$ is defined as

$$\Psi_{t}(i) = \begin{bmatrix} \lambda_{1}^{t} \psi_{1}(i) \\ \lambda_{2}^{t} \psi_{2}(i) \\ \vdots \\ \lambda_{N}^{t} \psi_{N}(i) \end{bmatrix}, \quad i = 1, \dots, N$$

$$(4)$$

where t is the scale parameter. The set of vectors $\Psi_t = \{\Psi_t(i)\}_{i=1}^N$ is the diffusion map for parameter t. Each vector $\Psi_t(i)$ is an embedding of node v_i in a Euclidean space.

We note that in their paper Coifman and Lafon did not include $\lambda_1^t \psi_1(i)$ in the diffusion embedding vectors (4). This omission is due to the fact that for any t and any i, $\lambda_1^t \psi_1(i)$ is constant (see Proposition 1 part 3). We add this term for convenience.

The diffusion embedding vectors preserve the local geometry of the graph. In order to show this, Coifman and Lafon introduce the diffusion distance, $D_t^2(i,j)$, which is a distance on the data set. Formally, the diffusion distance is defined as [11], [12], [14]

$$D_t^2(i,j) = \sum_{m=1}^{N} \frac{(p_t(x_i, x_m) - p_t(x_j, x_m))^2}{\phi_0(m)}$$
 (5)

where $p_t(x_a, x_b)$ is the probability of transition from node x_a to node x_b in t steps, and ϕ_0 is the leading left eigenvector of the Markov matrix. It can be shown that ϕ_0 is the stationary distribution of the Markov chain [12],

$$\phi_0(i) = \frac{d(v_i)}{\sum_{l=1}^{N} d(v_l)}.$$
 (6)

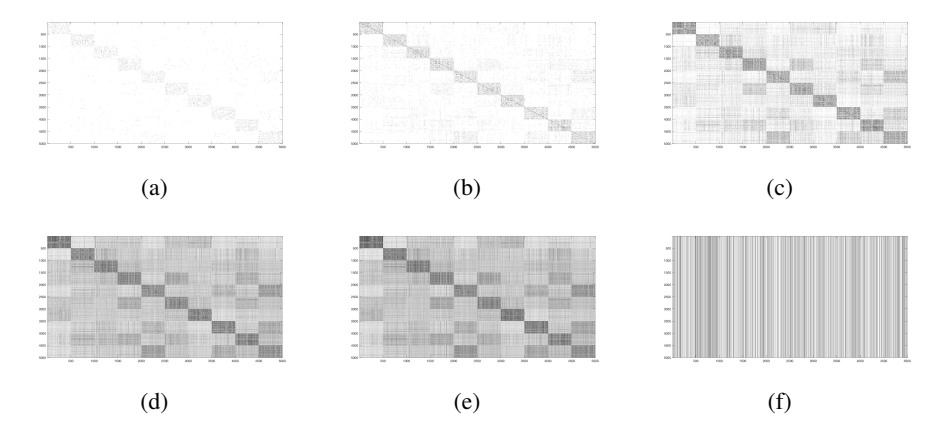


Fig. 1. Powers of the Markov matrix. Large transition probabilities are represented by dark pixels. Low probabilities of transition are represented by light pixels. (a) The Markov matrix \mathbf{P} . (b) \mathbf{P}^2 . (c) \mathbf{P}^4 . (d) \mathbf{P}^8 . (e) \mathbf{P}^{12} . (f) \mathbf{P}^{1024} .

For simplicity, we denote

$$d\left(\mathcal{G}\right) = \sum_{l=1}^{N} d\left(v_{l}\right).$$

The diffusion distance can then be expressed as

$$D_t^2(i,j) = \sum_{m=1}^N \left(\left(\mathbf{P}^t \right)_{i,m} - \left(\mathbf{P}^t \right)_{j,m} \right)^2 \cdot \frac{d(\mathcal{G})}{d(v_m)}. \quad (7)$$

If two nodes, v_i and v_j , have many short paths connecting them, then the probability of transition between them $(P_{i,j}^t)$ will be high. This means that the probability of each of these nodes transitioning to some general node v_m is similar, causing a low diffusion distance $D_t^2(i,j)$. On the other hand, if v_i and v_j are relatively disconnected, then the probability of each node transitioning to some general node v_m is different, causing the diffusion distance to be high. In this way the diffusion distance contains the connectivity information of the graph.

It can be shown that [11]

$$D_t^2(i,j) = \|\Psi_t(i) - \Psi_t(j)\|_2^2,$$
 (8)

where $\Psi_t(i)$ are defined in (4). Thus, the ℓ_2 distance between diffusion embedding vectors contains connectivity information of the graph. In other words, nodes that are strongly connected in the graph are given close (in the ℓ_2 sense) diffusion embedding vectors. Therefore, the diffusion map embedding Ψ_t preserves the local geometry of the graph at scale t.

Using the spectral properties of the Markov matrix, we can show that the dimension of the diffusion embedding vectors may be reduced while still preserving the local geometry of the graph. Noting that the diffusion distance can be written as

$$D_{t}^{2}(i, j) = \|\Psi_{t}(i) - \Psi_{t}(j)\|_{2}^{2}$$

$$= \sum_{m=1}^{N} \lambda_{m}^{2t} (\psi_{m}(i) - \psi_{m}(j))^{2}$$

$$= \sum_{m=2}^{N} \lambda_{m}^{2t} (\psi_{m}(i) - \psi_{m}(j))^{2}.$$
(9)

Since the magnitude of the eigenvalues decays to zero for many graphs that represent real life data sets, the dimension of the diffusion map embedding (for a known t) can be reduced by preserving only the entries of $\Psi_t(i)$ with the largest magnitude eigenvalues. Removing the diffusion coordinates associated with the smallest magnitude eigenvalues will not greatly effect $D_t^2(v_i,v_j)$. This dimension reduction is equivalent to discarding the eigenvectors with smallest eigenvalues.

We demonstrate the diffusion distances using the reduced MNIST data set. We choose a suitable kernel k (for example a Gaussian kernel) with the goals of differentiating between different digits while keeping the number of edges small. Figure 2 depicts the diffusion distances between each two nodes in the graph. We use the first 100 entries of $\Psi_t(i)$ for each node v_i , at scales t=0,4,8,12. It is clear from Fig. 2 that the diffusion distances between two nodes in the same cluster (two nodes representing images of the same digit) are lower than the diffusion distances between two nodes in different clusters.

Diffusion maps have been used in many applications, among them dimension reduction [11], clustering [13], sensor localization [12], data fusion [15] and speech enhancement [14].

C. Signals Processing on Graphs

As in diffusion maps, in the field of signal processing on graphs a data set is represented by a weighted graph. The goal is to extend of operations and results of signal processing to signals defined on this graph.

A signal over a graph is defined in the literature as a mapping from each node v_i to a real or complex scalar value s_i [4], [5], [6], [9]. Some works in this field use weighted undirected graphs with non-negative weights [3], while others use more general graphs having either directed or undirected edges for data representation [4], [5], [6].

The pairwise (edge) information of the graph is contained in the graph shift operator A [4]. The graph shift operator is a weighted adjacency matrix where the ijth entry corresponds to the pairwise relationship between nodes v_i and v_j . When nodes v_i and v_j are not adjacent (i.e. not connected by an

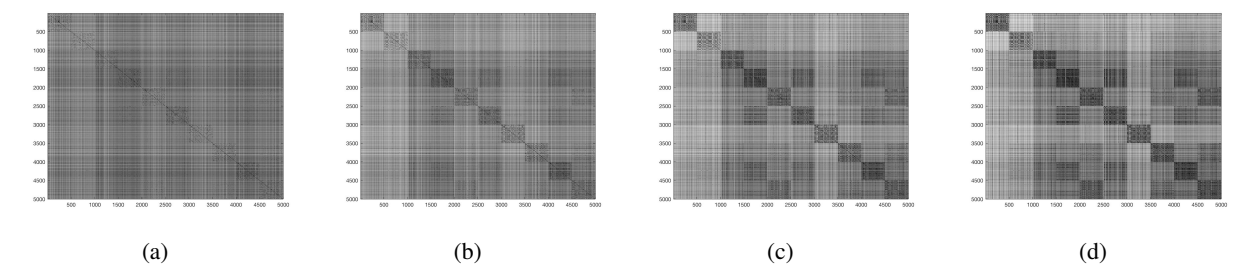


Fig. 2. Diffusion distances. Short distances are represented by dark pixels. Long distances are represented by light pixels. (a) Distances at scale t = 0. (b) Distances at scale t = 4. (c) Distances at scale t = 8. (d) Distances at scale t = 12.

edge), $A_{i,j} = 0$. Otherwise $A_{i,j}$ contains the weight of an edge originating at node v_i and terminating at node v_j .

The graph shift operation [5] is defined as

$$\tilde{\mathbf{s}} = \mathbf{A}\mathbf{s}.\tag{10}$$

This operation redistributes the graph signal at each node according to its neighborhood and is a generalization of time shifts [4]. Let the graph \mathcal{G} represent a uniformly sampled periodic time series. In this case, each node of the graph is adjacent to a single neighbor, and the graph shift operator is

$$\mathbf{A} = \begin{bmatrix} 0 & 1 & 0 & 0 & \cdots \\ 0 & 0 & 1 & 0 & \cdots \\ \vdots & \vdots & \vdots & \vdots & \ddots \\ 1 & 0 & 0 & 0 & \cdots \end{bmatrix}. \tag{11}$$

The graph shift then results in

$$\mathbf{A}\mathbf{s} = \tilde{\mathbf{s}} = \begin{bmatrix} s_2 \\ s_3 \\ \vdots \\ s_N \\ s_1 \end{bmatrix}. \tag{12}$$

Based on this definition of the graph shift, Sandryhaila and Maura introduce the linear shift invariant graph filter [5]

$$H(\mathbf{s}) = h_0 \mathbf{s} + h_1 \mathbf{A} \mathbf{s} + \dots + h_L \mathbf{A}^L \mathbf{s}. \tag{13}$$

The graph shift operator is also used in the definition of the graph Fourier transform (GFT) [4], which is defined as

$$\hat{\mathbf{s}} = \mathbf{V}^{-1}\mathbf{s}.\tag{14}$$

If the graph shift is diagonalizable then V is the matrix containing in its columns the eigenvectors of the graph shift operator. Otherwise, V is the matrix containing in its columns the generalized eigenvectors of the graph shift operator. The vector $\hat{\mathbf{s}}$ is the spectrum of the graph signal. When this spectrum contains k nonzero entries, we say that the graph signal is k-bandlimited [6]. The inverse graph Fourier transform (IGFT) is given by

$$\mathbf{s} = \mathbf{V}\hat{\mathbf{s}}.\tag{15}$$

The GFT can be interpreted as a generalization of the Fourier transform. When the graph represents a periodic time series, the graph shift operator is circulant and thus the matrix containing its eigenvectors is the DFT matrix.

The graph shift operator is very important to the field of signal processing on graphs. However, its definition as a weighted adjacency matrix is not unique. In Section IV we suggest defining the graph shift operator as the Markov matrix of (1). In Section V we present several advantages to this definition.

III. SIGNALS OVER GRAPHS

The definition of a graph signal as a mapping from each node to a real or complex scalar value [4], [5], [6], [9] disconnects the graph signal from the graph. It allows any vector in \mathbb{R}^N to be a graph signal residing over any graph with N nodes, irrespective of the graph's structure. We suggest an alternative definition of the graph signal, which relies on the ℓ_2 distances between the diffusion map embeddings of strongly connected nodes in the graph.

Definition 1. A graph signal is a mapping from each node v_i to a real or complex scalar value s_i , such that the geometry of the graph is adhered to.

Adherence to the graph geometry is manifested via a smoothness constraint, requiring that the graph signal is smooth over the edges of the graph. Thus, a graph signal is a mapping from each node v_i to a real or complex scalar value s_i , such that the vector $\mathbf{s} = \begin{bmatrix} s_1 & \cdots & s_N \end{bmatrix}^T \in \mathbb{C}^N$ is smooth over the graph. Under this definition, the geometry of the graph will contain information about the graph signal, and the graph signal contains geometric information. In fact, Dong *et al.* [7] show that the graph topology can be learned from a smooth graph signal¹.

Several smoothness measures for graph signals have been suggested in prior literature. In [5], the authors define the total variation of a graph as

$$TV(\mathbf{s}) = \|\mathbf{s} - \tilde{\mathbf{A}}\mathbf{s}\|_{p} \tag{16}$$

where $\tilde{\mathbf{A}}$ is a normalization of the graph shift operator (the weighted adjacency matrix) such that the largest magnitude eigenvalue is equal to one. An alternative smoothness measure, related to edge derivatives [7], [10], is given by

$$\mathbf{s}^{T} \mathcal{L} \mathbf{s} = \frac{1}{2} \sum_{i=1}^{N} \sum_{m=1}^{N} W_{i,m} (s_{i} - s_{m})^{2}$$
 (17)

¹We note that, in contrast to our definition, Dong *et al.* consider smooth graph signals to be a subclass of general graph signals.

where \mathbf{W} is the symmetric affinity matrix and \mathcal{L} is the unnormalized graph Laplacian $\mathcal{L} = \mathbf{D} - \mathbf{W}$.

We introduce the Markov variation, a smoothness measure which bears some similarity to both (16) and (17), while offering a probabilistic interpretation. To motivate the Markov variation, consider a graph signal $s \in \mathbb{R}^N$. Since s should map closely connected nodes to similar values, we can think of the graph signal at the nodes neighboring v_i (i.e. $\{s_j\}_{j\in\mathcal{N}_i}$) as defining a distribution over s_i . We then model s_i as

$$s_{i} = \sum_{m \in \mathcal{N}_{i}} P_{i,m} s_{m} + \epsilon \left(s_{i} \right), \tag{18}$$

where **P** is the Markov transition matrix, \mathcal{N}_i is the set of nodes adjacent to v_i and ϵ is an error term.

The model in (18) consists of two terms. The first is an estimate of the graph signal s_i based only on the neighboring nodes and transition probabilities. This is a Markovian model, where the assumption is that when the graph signals at neighboring nodes are known, there is no dependence on non-neighboring nodes. Since we define the graph signal as a mapping that conforms to the geometry of the graph, the transition probabilities between two neighboring nodes can be thought of as an approximation of the probability of both nodes having the same graph signal. Thus, for any graph signal s we expect $s_i - \sum_{m \in \mathcal{N}_i} P_{i,m} s_m$ to be small. This difference corresponds to the second term in (18) which is an error term ϵ that explains variations from the weighted sum of neighbors.

The Markov variation is the norm of the error term

$$\|\epsilon(\mathbf{s})\|_{p} = \|\mathbf{s} - \mathbf{P}\mathbf{s}\|_{p}.\tag{19}$$

For example, using the ℓ_1 norm we obtain

$$\|\mathbf{s} - \mathbf{P}\mathbf{s}\|_{1} = \sum_{i=1}^{N} \frac{1}{d(v_{i})} \left| \sum_{m=1}^{N} W_{i,m}(s_{i} - s_{m}) \right|.$$
 (20)

We then define a graph signal as a vector $\mathbf{s} \in \mathbb{R}^N$ with low Markov variation, *i.e.*,

$$\|\mathbf{s} - \mathbf{P}\mathbf{s}\|_{p} < e,\tag{21}$$

where e is determined according the number of nodes in the graph.

The advantage of the Markov variation over total variation is easily demonstrated for a static graph signal. Due to the probabilistic nature of the Markov variation, when the vector of graph signals is a constant vector, $\|\mathbf{s} - \mathbf{P}\mathbf{s}\|_p = \|\mathbf{0}\|_p = 0$. This is not necessarily true for (16). Thus, the fact that each row of the matrix \mathbf{P} sums to one is an advantage over the total variation measure.

Next, we compare the Markov variation with (17). In both (17) and (20) the smoothness measure is a sum over all nodes. This sum takes into account the smoothness at each node. The advantage of the Markov variation stems from the fact that the measure of (17) considers $(s_i - s_m)^2$ and does not take into account whether $s_i \leq s_m$ or $s_i \geq s_m$. In order to demonstrate the difference between these cases, we consider two scenarios. In the first scenario node v_i has six neighbors, three of which have a graph signal of $s_i + \alpha$ and three of which have a graph signal of $s_i - \alpha$, where $\alpha \in \mathbb{R}$. In the second case node v_i

has six neighbors, all of which have a graph signal of $s_i + \alpha$. These cases are not the same, however they will have the same smoothness in (17). In contrast, the difference between these cases is manifested in the Markov variation measure as well as the total variation measure.

An interesting property of the Markov variation is that it expresses an equivalence between smoothness measured over the edges of the graph and smoothness measured over diffusion embedding vectors. Since from Lemma 1 the Markov matrix is diagonalizable, (19) can be written as

$$\|\mathbf{s} - \mathbf{P}\mathbf{s}\|_{p} = \|\mathbf{s} - \mathbf{V}\mathbf{\Lambda}\mathbf{V}^{-1}\mathbf{s}\|_{p}$$
 (22)

where Λ is a diagonal matrix that contains the eigenvalues of the Markov matrix. From (14) and (15) we have

$$\|\mathbf{s} - \mathbf{P}\mathbf{s}\|_p = \|\mathbf{s} - \mathbf{V}\mathbf{\Lambda}\mathbf{V}^{-1}\mathbf{s}\|_p = \|\mathbf{V}\hat{\mathbf{s}} - \mathbf{V}\mathbf{\Lambda}\hat{\mathbf{s}}\|_p.$$
(23)

The rows of $\Psi_t = \mathbf{V} \mathbf{\Lambda}^t$ contain the diffusion embedding vectors of the graph. For example, the *i*th row equals

$$\Psi_t^T(i) = \begin{bmatrix} \lambda_1^t \psi_1(i) & \lambda_2^t \psi_2(i) & \cdots & \lambda_N^t \psi_N(i) \end{bmatrix}. \quad (24)$$

The ℓ_p norm of (21) can thus be expressed as

$$\|\mathbf{s} - \mathbf{P}\mathbf{s}\|_{p}^{p} = \sum_{i=1}^{N} |\left(\Psi_{0}(i)^{T} - \Psi_{1}^{T}(i)\right)\hat{\mathbf{s}}|^{p} < e^{p},$$
 (25)

which relates the spectrum of a graph signal with the diffusion embedding vectors.

We conclude that on the one hand the Markov variation can be expressed as a connection between the graph signal and the geometry of the graph (19) in the graph domain. On the other hand, the smoothness function can be expressed as a connection between the spectrum of the graph signal and the diffusion embedding vectors in the frequency domain. In addition, (25) can be rewritten as

$$\|\mathbf{s} - \mathbf{P}\mathbf{s}\|_{p}^{p} = \sum_{i=1}^{N} |s_{i} - \Psi_{1}^{T}(i)\,\hat{\mathbf{s}}|^{p} < e^{p},$$
 (26)

which implies that for a vector s to be a graph signal, s_i must be close to s_j if $\Psi_1(i)$ and $\Psi_1(j)$ are close (in the ℓ_2 sense). Another important conclusion can be obtained from

$$\|\mathbf{s} - \mathbf{P}\mathbf{s}\|_{p}^{p} = \|\mathbf{V}(\mathbf{I}_{N} - \mathbf{\Lambda})\,\hat{\mathbf{s}}\|_{p}^{p} < e^{p}.$$
 (27)

Since the largest eigenvalue of the Markov matrix is 1 (see Proposition 1 part 2) and the magnitude of the smaller eigenvalues is often 0, the entries of \$\hat{s}\$ that are related to the highest eigenvalues do not contribute much to the sum (27). The entries of \$\hat{s}\$ that correspond to the lower eigenvalues have a higher impact on the sum (27). This means that, in order for a signal s to be a graph signal, many of the entries of \$\hat{s}\$ that correspond to the lower valued eigenvalues must be negligible. In other words, the spectrum of a graph signal is sparse. We will use this property in Section V-A for graph signal interpolation.

IV. CONNECTING SP ON GRAPHS AND DIFFUSION MAPS

While the graph shift operator is very important to the field of signal processing on graphs, its definition as a weighted adjacency matrix is not unique. We define the graph shift operator to be the Markov matrix

$$\mathbf{A} = \mathbf{P},\tag{28}$$

which is possible since the Markov matrix contains information about pairwise relationships in the graph and is thus a weighted adjacency matrix. We note that under this definition the graph shift operation will redistribute the graph signal according to the transition probabilities of a Markov chain defined on the graph. For node v_i , the shift operation will result in $\sum_{m=1}^{N} P_{i,m} s_m$.

Below, we show the connection between signal processing on graphs and diffusion maps emerging from (28). For consistency with diffusion maps we use weighted undirected graphs with non-negative weights to represent data. Similar constraints were used in [3]. In general graph weights are very often modeled as non-negative [16].

We next examine the graph shift operation resulting from (28). The diffusion maps framework defines an embedding for the nodes of the graph with a time-scale parameter t. The graph shift operation is strongly related to shifting the time-scale parameter,

$$\mathbf{s} = \mathbf{V}\hat{\mathbf{s}} = \mathbf{\Psi}_0\hat{\mathbf{s}},$$

$$\mathbf{A}^T\mathbf{s} = \mathbf{V}\mathbf{\Lambda}^T\hat{\mathbf{s}} = \mathbf{\Psi}_T\hat{\mathbf{s}}.$$
(29)

where ${\bf V}$ is the matrix of eigenvectors of the graph shift operator. Thus the graph shift operation can be interpreted as a shift in the family of embeddings, for example from $\{\Psi_0\}$ to $\{\Psi_T\}$.

The connection between graph filters and diffusion maps using (30) is based on the connection between the graph shift operation and the diffusion maps framework. A linear shift invariant graph filter [5] is defined as

$$H(\mathbf{s}) = h_0 \mathbf{s} + h_1 \mathbf{A} \mathbf{s} + \dots + h_L \mathbf{A}^L \mathbf{s}.$$
 (30)

Combining (30) with (29) we have

$$H(\mathbf{s}) = h_0 \mathbf{\Psi}_0 \hat{\mathbf{s}} + h_1 \mathbf{\Psi}_1 \hat{\mathbf{s}} + \dots + h_L \mathbf{\Psi}_L \hat{\mathbf{s}}. \tag{31}$$

We conclude that the graph filter looks at several scales of diffusion embeddings. Thus, the output considers the pairwise relationship between nodes in the graph at several scales.

V. ADVANTAGES OF USING THE MARKOV MATRIX AS THE GRAPH SHIFT

In this section we will present several advantages of the choice A = P.

A. Semi-Supervised Learning of Graph Signals

We have seen that the diffusion map embedding preserves the local geometry of the graph. Closely connected nodes in the graph have close (in the ℓ_2 sense) diffusion embedding vectors. Usually the actual distance between far apart data elements is meaningless [11], so an embedding that preserves the local geometry is a good representation of the data set (provided that the graph is a good representation of the data set). This allows us to dispose of the graph and view the graph signal as a mapping from the set of diffusion embedding vectors to some scalar. Close diffusion embedding vectors (in the ℓ_2 sense) will be mapped to similar real or complex scalar values.

Viewing the graph signal as a function over the diffusion embedding vectors is an advantage since it allows the signal processing to be performed over a Euclidean space. In practice, as the diffusion embedding vectors preserve the local geometry of the graph, the processing is still on the graph.

To illustrate this point, we consider the problem of semi-supervised learning of graph signals, where the signals over r nodes of the graph are known a-priori. Let the set $\mathcal M$ be a sampling set containing the indices of these r nodes, and denote the vector of known graph signals as $\mathbf s_{\mathcal M} \in \mathbb R^{r \times 1}$. The goal is to recover $\mathbf s$ from $\mathbf s_{\mathcal M}$ and the known graph structure.

We aim to solve this problem over the diffusion embedding vectors. Since the graph structure is known, the diffusion embedding vectors can all be computed. We know from the smoothness property of graph signals and (25) that for each node i,

$$s_i \approx \Psi_1^T(i)\,\hat{\mathbf{s}}.$$
 (32)

If the signal s is the smoothest possible signal according to the Markov variation (*i.e.*, the error term is 0), then

$$s_i = \Psi_1^T(i)\,\hat{\mathbf{s}},\tag{33}$$

which leads to the following system of equations

$$\begin{bmatrix} s_1 \\ s_2 \\ \vdots \\ s_N \end{bmatrix} = \begin{bmatrix} \lambda_1 \psi_1 (1) & \lambda_2 \psi_2 (1) & \cdots & \lambda_N \psi_N (1) \\ \lambda_1 \psi_1 (2) & \lambda_2 \psi_2 (2) & \cdots & \lambda_N \psi_N (2) \\ \vdots & \vdots & \ddots & \vdots \\ \lambda_1 \psi_1 (N) & \lambda_2 \psi_2 (N) & \cdots & \lambda_N \psi_N (N) \end{bmatrix} \begin{bmatrix} \hat{s}_1 \\ \hat{s}_2 \\ \vdots \\ \hat{s}_N \end{bmatrix}.$$
(34)

Out of these N equations, we examine those that correspond to the known graph signals

$$\mathbf{s}_{\mathcal{M}} = \begin{bmatrix} \lambda_1 \psi_1 (\mathcal{M}) & \lambda_2 \psi_2 (\mathcal{M}) & \cdots & \lambda_N \psi_N (\mathcal{M}) \end{bmatrix} \hat{\mathbf{s}} \quad (35)$$

where $\psi_i(\mathcal{M})$ is a sub-vector of the diffusion embedding vector of node v_i , containing only the entries at the set of indices \mathcal{M} .

The solution of (35) is not unique. One such solution is for example least squares. However, since the eigenvalues of the Markov matrix often decay to 0 for real-life datasets, we concluded in Section III that the spectrum of the graph signal is sparse. Thus, we search for the subset of eigenvectors of the Markov matrix that best explain the known portion of the

graph signal, and arrive at the following sparse optimization problem

$$\hat{\mathbf{s}} = \arg\min_{\mathbf{y}} \|\mathbf{y}\|_{0} \quad \text{such that}$$

$$\left[|\lambda_{1}\psi_{1}(\mathcal{M}) \quad \lambda_{2}\psi_{2}(\mathcal{M}) \quad \cdots \quad \lambda_{N}\psi_{N}(\mathcal{M}) \right] \mathbf{y} = \mathbf{s}_{\mathcal{M}}.$$
(36)

This optimization problem searches for the spectrum of the smoothest possible signal that contains the known portion of the graph signal. In practice we allow a small tolerance for error in accordance with (32). An approximate solution of (36) can be obtained through ℓ_1 minimization. The vector of graph signals is obtained by inserting the solution to (36) into (34).

This example of semi-supervised learning demonstrates an advantages to the definition of the graph shift operator as the Markov matrix, which stems from the fact that the geometric information is mostly contained in a subset of eigenvectors and eigenvalues of the Markov matrix. Since the graph signal must adhere to the geometry of the graph, this property allows to search for a sparse spectrum \hat{s} that best explains the known portion of the graph signal.

We note that when the graph shift operator is the Markov matrix, existing diffusion map frameworks can be used for processing signals over graphs. Indeed, the framework suggested in this section is an extension, or a slight variation, on the existing spectral regression framework [12], which is a diffusion map based framework that was suggested by Keller and Gur as a solution to the sensor localization problem. Thus, defining the graph shift operator as the Markov matrix allows to incorporate data processing methods developed for diffusion maps into the field of signal processing on graphs.

A related problem to semi-supervised learning was considered in [6]. There the authors present a sampling theory for K-bandlimited graph signals. The goal of their work is to allow perfect reconstruction of such graph signals from K samples. To this end they discuss which nodes should be sampled in order to allow perfect reconstruction. We note that, when the graph shift operator is the Markov matrix, spectral regression also leads to perfect reconstruction for K-bandlimited graph signals under the sampling specified in [6]. Specifically, while in general the solution of (35) is not unique, in the case of a K-bandlimited graph signal the solution may be unique. Denoting the set of indices of the nonzero elements of $\hat{\mathbf{s}}$ by \mathcal{A} , (35) can be rewritten as

$$\mathbf{s}_{\mathcal{M}} = \begin{bmatrix} \lambda_{\mathcal{A}_{1}} \psi_{\mathcal{A}_{1}} \left(\mathcal{M} \right) & \cdots & \lambda_{\mathcal{A}_{K}} \psi_{\mathcal{A}_{K}} \left(\mathcal{M} \right) \end{bmatrix} \hat{\mathbf{s}}. \tag{37}$$

Assuming the K eigenvalues are nonzero, the K columns of the matrix in (37) are linearly independent. Under the sampling suggested in [6], the rows of this matrix will also be linearly independent, and thus there will exist a unique solution.

B. Big Data

The spectral regression framework necessitates computation of the eigendecomposition of the graph shift operator. This computation is costly in terms of both complexity and memory consumption. When the graph has $N\gg 1$ nodes, it may not be feasible to compute eigenvectors and eigenvalues of the

graph shift operator. However, when the graph shift operator is the Markov matrix, a variation on the Nyström extension [17], [18], [19], [20] can be used for semi-supervised learning of big data.

We begin by giving a short introduction to the Nyström extension. Let $\{\mathbf{x}_i\}_{i=1}^N$ be a set of data points. A matrix $\mathbf{K} \in \mathbb{R}^{N \times N}$ is constructed such that $K_{i,j} = k(\mathbf{x}_i, \mathbf{x}_j)$, where $k(\cdot)$ is some kernel function and \mathbf{K} is a positive semi-definite (PSD) matrix. The matrix \mathbf{K} can be considered as a combination of four block matrices,

$$\mathbf{K} = \begin{bmatrix} \mathbf{E} & \mathbf{B}^T \\ \mathbf{B} & \mathbf{C} \end{bmatrix},\tag{38}$$

where $\mathbf{E} \in \mathbb{R}^{r \times r}$, $\mathbf{B} \in \mathbb{R}^{N-r \times r}$, and $\mathbf{C} \in \mathbb{R}^{N-r \times N-r}$ for some 0 < r < N. The Nyström extension is a method for extending the eigenvectors of \mathbf{E} to create an estimate of r eigenvectors of \mathbf{K} .

Let $\mathbf{Z} \in \mathbb{R}^{r \times r}$ be the matrix whose columns are the eigenvectors of \mathbf{E} . As \mathbf{E} contains the first r rows and the first r columns of \mathbf{K} , it is itself a symmetric matrix, thus

$$\mathbf{E} = \mathbf{Z}\mathbf{Q}\mathbf{Z}^T \tag{39}$$

where \mathbf{Q} is a diagonal matrix containing the eigenvalues of \mathbf{E} . The Nyström extension of the matrix of eigenvectors of \mathbf{K} is given by

$$\tilde{\mathbf{Z}} = \begin{bmatrix} \mathbf{Z} \\ \mathbf{B}\mathbf{Z}\mathbf{Q}^{-1} \end{bmatrix}. \tag{40}$$

For more details see [17].

The Nyström extension (40) contains a division by eigenvalues. Due to this division there may be numerical instabilities, causing some of the eigenvectors to have very large values in the $(r+1),\ldots,N$ coordinates. This will cause the spectral regression scheme to fail since the graph signal will be determined by the large valued eigenvectors instead of the known graph signals. We thus suggest to change the extension as follows:

$$\tilde{\mathbf{Z}} = \begin{bmatrix} \mathbf{Z} \\ \mathbf{B}\mathbf{Z} \end{bmatrix}. \tag{41}$$

We justify the exclusion of \mathbf{Q}^{-1} below. In particular, we show that this leads to an efficient graph interpolation method (see (56) below) which does not require computing any eigenvalues or eigenvectors but relies only on the values at the given nodes.

The application of the Nyström extension to the Markov matrix is not straightforward. This is due to the fact that the Nyström extension is geared towards PSD matrices, and the Markov matrix **P** is not a PSD matrix. However, the Markov matrix is strongly related to the normalized graph Laplacian **L** which is PSD, and defined by

$$\mathbf{L} = \mathbf{D}^{-\frac{1}{2}} (\mathbf{D} - \mathbf{W}) \mathbf{D}^{-\frac{1}{2}} = \mathbf{I}_{N} - \mathbf{D}^{-\frac{1}{2}} \mathbf{W} \mathbf{D}^{-\frac{1}{2}}$$
(42)

where \mathbf{I}_N is the $N \times N$ identity matrix. It is easy to see that $\mathbf{D}^{-\frac{1}{2}}\mathbf{L}\mathbf{D}^{\frac{1}{2}} = \mathbf{I}_N - \mathbf{P}$. Thus, the normalized graph Laplacian is similar to $\mathbf{I}_N - \mathbf{P}$. The connection between the matrix of eigenvectors of the Markov matrix \mathbf{V} and the matrix of eigenvectors of the Laplacian \mathbf{U} is then

$$\mathbf{V} = \mathbf{D}^{-\frac{1}{2}}\mathbf{U}.\tag{43}$$

In addition, the diagonal matrix containing the eigenvalues of the Markov matrix Λ and the diagonal matrix containing the eigenvalues of the Laplacian $\bar{\Lambda}$ are related by

$$\mathbf{\Lambda} = \mathbf{I}_N - \bar{\mathbf{\Lambda}}.\tag{44}$$

We note that (43) and (44) are the vector form of Proposition 1 part 1. Their proof is given in the appendix.

To obtain an efficient graph signal interpolation algorithm we would like to use the approximate eigenvectors and eigenvalues of ${\bf P}$ for spectral regression (36). To this end, we estimate the eigendecomposition of the Laplacian via the Nyström extension, and then approximate the eigendecomposition of the Markov matrix via (43) and (44). This allows us to reduce the computational complexity of spectral regression for data sets with many elements. Once the eigenvectors of the Laplacian are recovered, the eigenvectors of the Markov matrix ${\bf P}$ can be found as follows,

$$V_{a,i} = \frac{1}{\sqrt{d(a)}} \tilde{U}_{a,i}, \quad 1 \le a \le N$$

$$\tag{45}$$

where V is the matrix containing the estimated eigenvectors of the Markov matrix, and $d\left(a\right)$ is the degree of node v_a . The diagonal matrix containing the eigenvalues of the Markov matrix can be estimated as

$$\mathbf{\Lambda} = \mathbf{I}_r - \mathbf{Q}.\tag{46}$$

In order to see that the graph signal interpolation can be solved via spectral regression using the approximated eigenvectors and eigenvalues, we rewrite (32) as

$$s_{i} \approx \sum_{i=1}^{N} \lambda_{j} \psi_{j} (i) \,\hat{s}_{j}. \tag{47}$$

Since the Nyström extension provides an estimate of the first r eigenvectors and eigenvalues of \mathbf{P} , we approximate the graph signal as

$$\bar{s}_i = \sum_{j=1}^r (1 - Q_{j,j}) \, \tilde{\mathbf{z}}_j \, (i) \, \hat{s}_j,$$
 (48)

where $\tilde{\mathbf{z}}_j$ and \bar{s}_i are estimates of ψ_j and s_i , respectively.

For the known portion of the graph signal, $\bar{\mathbf{s}}_{\mathcal{M}}$ must equal $\mathbf{s}_{\mathcal{M}}$. We thus arrive at a set of $|\mathcal{M}|$ equations with r unknown. The solution of the system is not unique when we choose a value of r that is higher than the cardinality of \mathcal{M} . We can therefore use the spectral regression solver on the following optimization problem

$$\mathbf{x} = \arg\min_{\mathbf{y}} \|\mathbf{y}\|_{0} \quad \text{such that}$$

$$\left[(1 - Q_{1,1}) \,\tilde{\mathbf{z}}_{1} \,(\mathcal{M}) \quad \cdots \quad (1 - Q_{r,r}) \,\tilde{\mathbf{z}}_{r} \,(\mathcal{M}) \right] \mathbf{y} = \mathbf{s}_{\mathcal{M}}. \tag{49}$$

The graph signal is then estimated by (48).

So far we assumed that N-r frequencies of the graph signal equal 0. We now add an additional assumption, namely $r=|\mathcal{M}|$, which will allow us to develop a closed form expression for interpolation of graph signals from the inverse GFT

$$\mathbf{s} = \mathbf{V}\hat{\mathbf{s}} = \mathbf{D}^{-\frac{1}{2}}\mathbf{U}\hat{\mathbf{s}}.\tag{50}$$

Since there are $|\mathcal{M}|=r$ nodes with a known graph signal, we suggest to index these nodes as v_1,\ldots,v_r (i.e. $\mathcal{M}=\{1,\ldots,r\}$). This is possible since when building the graph, indices are arbitrarily assigned to nodes. The suggested indexing will associate the sub-matrix \mathbf{E} with the sampling set \mathcal{M} . To show this, we examine the normalized graph Laplacian \mathbf{L} ,

$$L_{j,i} = L_{i,j} = \begin{cases} -\frac{W_{i,j}}{\sqrt{d(i)d(j)}} & i \neq j\\ 1 & i = j. \end{cases}$$
 (51)

We see that each node v_i is associated with the *i*th row and with the *i*th column of the Laplacian. This will cause the first n rows and columns of the Laplacian to be associated with nodes v_1, \ldots, v_r . Thus, the matrix \mathbf{Z} is the exact eigenvectors computed from the sub-matrix of the portion of the Laplacian that is associated with the set \mathcal{M} .

After extending the eigenvectors, we arrive at the matrix **Z** (41) which is of size $N \times r$. We denote the vector containing the first r frequencies of the graph signal as \mathbf{x} . Replacing the matrix \mathbf{U} in (50) with our approximation, we arrive at the following approximation of the graph signal,

$$\bar{\mathbf{s}} = \mathbf{D}^{-\frac{1}{2}} \begin{bmatrix} \mathbf{Z} \\ \mathbf{BZ} \end{bmatrix} \mathbf{x}.$$
 (52)

The matrix $\mathbf{D}^{-\frac{1}{2}}$ can be represented as a block matrix,

$$\mathbf{D} = \begin{bmatrix} \mathbf{D}_e & \mathbf{0} \\ \mathbf{0} & \mathbf{D}_b \end{bmatrix},\tag{53}$$

where \mathbf{D}_e is of size $r \times r$ and \mathbf{D}_b is of size $N - r \times N - r$. It follows that

$$\bar{\mathbf{s}} = \mathbf{D}^{-\frac{1}{2}} \begin{bmatrix} \mathbf{Z} \\ \mathbf{B} \mathbf{Z} \end{bmatrix} \mathbf{x} = \begin{bmatrix} \mathbf{D}_e^{-\frac{1}{2}} \mathbf{Z} \mathbf{x} \\ \mathbf{D}_h^{-\frac{1}{2}} \mathbf{B} \mathbf{D}_e^{\frac{1}{2}} \mathbf{D}_e^{-\frac{1}{2}} \mathbf{Z} \mathbf{x} \end{bmatrix}.$$
(54)

If we had not used the approximate eigenvectors, the first r entries of $\bar{\mathbf{s}}$ would equal the sampled graph signals. Thus, we substitute

$$\mathbf{D}_e^{-\frac{1}{2}}\mathbf{Z}\mathbf{x} \approx \mathbf{s}_{\mathcal{M}} \tag{55}$$

in (54), and arrive at

$$\bar{\mathbf{s}} = \begin{bmatrix} \mathbf{D}_e^{-\frac{1}{2}} \mathbf{Z} \mathbf{x} \\ \mathbf{D}_b^{-\frac{1}{2}} \mathbf{B} \mathbf{D}_e^{\frac{1}{2}} \mathbf{D}_e^{-\frac{1}{2}} \mathbf{Z} \mathbf{x} \end{bmatrix} \approx \begin{bmatrix} \mathbf{s}_{\mathcal{M}} \\ \mathbf{D}_b^{-\frac{1}{2}} \mathbf{B} \mathbf{D}_e^{\frac{1}{2}} \mathbf{s}_{\mathcal{M}} \end{bmatrix}.$$
(56)

This enforces smoothness of the graph signal. The graph signal at node v_i is a linear combination of the known portion of the graph signal of the nodes in the neighborhood of v_i . The contribution of each neighbor v_j depends upon three factors. The first is similarity between v_i and v_j (i.e., the matrix B). The second factor is the degree of node v_i . If v_i has many neighbors, then less weight is given to each neighbor. The third factor is the degree of node v_j . If v_j is a central node, then it is given higher weight.

In addition to solving the problem of numerical instability while enforcing the smoothness of the graph signal, the variation (41) on the Nyström extension also provides a simple closed form expression for the interpolation of smooth graph signals when only the first r frequencies are nonzero. We note that no eigenvectors or eigenvalues actually need to be recovered.

VI. EXPERIMENTAL RESULTS FOR GRAPH SIGNAL INTERPOLATION

We present experimental results of the graph signal interpolation method presented in Section V-B. Our framework is verified using the MNIST data set of handwritten digits [1]. This data set includes 60000 training images and 10000 test images. The goal is to associate each image with the correct digit.

We formulate this problem as a graph signal interpolation problem. The dataset is represented via an undirected weighted graph, wherein each image x_i is represented by a single node v_i . We follow the practice suggested in [6], and set the distance $F_{i,j}$ between two nodes v_i and v_j as the Euclidean distances between vectorizations of the images they represent. The matrix containing all pairwise distances between nodes in the graph is denoted by \mathbf{F} .

Since we wish to preserve local distance, we keep only the 200 smallest entries for each row n in \mathbf{F} , while the remaining distances are set to infinity. The set of indices of the finite entries in row n is denoted as \mathcal{M}_n . We follow the practice suggested in [6], and set the weight of an edge between each two images to be

$$W_{i,j} = \begin{cases} \frac{F_{i,j} \cdot 70000^2}{\sum_{n=1}^{N} \sum_{m \in \mathcal{M}_n} F_{n,m}} & \text{for } j \in \mathcal{M}_i \\ 0 & \text{for } j \notin \mathcal{M}_i \end{cases}$$
 (57)

We then symmetrize this matrix as

$$W_{i,j} = \max(W_{i,j}, W_{j,i}).$$
 (58)

It should be noted that digit 1 is more similar to 4 than to 2. For this reason, a signal mapping each node to one of 10 digits may not be smooth over the graph. Due to this, we define ten graph signals s^0, \ldots, s^9 by

$$s_i^k = \begin{cases} 1 & \text{if } v_i \text{ represents an image of the digit } k, \\ 0 & \text{otherwise.} \end{cases}$$
 (59)

Each of these signals is smooth over the graph.

For graph signal interpolation, each graph signal is assumed to be known over a subset of r nodes in the training set. The goal is to recover the signals over the test set. This is done via (56). We will say that node v_i represents an image of digit k when $|s_i^k| > |s_i^m|$ for all $k \neq m$. This allows us to report an accuracy of interpolation for each value of r.

Figure 3 presents the accuracy and runtime of the graph signal interpolation framework presented in Section V-B. We compare the results of our variation on the Nyström extension to results from the spectral regression framework presented in Section V-A.

The spectral regression framework calculates the eigenvectors exactly. Since we cannot compute the eigendecomposition of a 70000×70000 Markov matrix, we extract the submatrix containing r randomly chosen (sampled) nodes from the training set and the 10000 nodes of the test set. Since an eigendecomposition of this smaller matrix is still substantially slower than the suggested approximation of Section V-B, we compute 20 eigenvectors of the sub-matrix for each value of r. This makes runtimes comparable between the methods

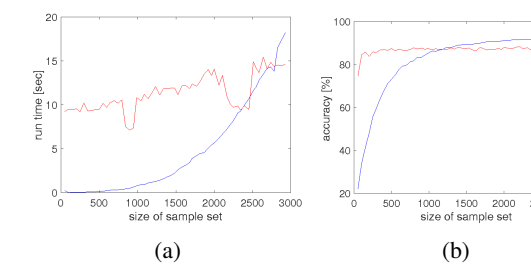


Fig. 3. Graph signal interpolation on the MNIST data set. Results for the Nyström based method are presented in blue. Results of Spectral Regression are presented in red. (a) size of training set (r) vs. rate of accurate graph signal reconstruction. (b) size of training set (r) vs. total time for graph signal reconstruction.

detailed in this paper. Spectral regression is solved using the SPGL1 package² [21], [22].

We note that in the Nyström-based interpolation, as the size of the training set (r) grows, the complexity of calculating (39) increases. In the Spectral Regression interpolation framework, as the size of the training set (r) grows so does the size of the graph shift. However, the number of calculated eigenvectors remains unchanged. Thus, when r=2600 runtime for both frameworks is approximately equal. In addition, at this value of r, the results of the Nyström-based interpolation are more accurate due to the limitation imposed on the number of eigenvalues computed in the Spectral Regression framework. In order to achieve comparable accuracy, the number of eigenvectors computed would need to be increased, causing an increase in runtime as well. In summary, our variation on the Nyström extension performs faster while still achieving good accuracy.

VII. CONCLUSION

The field of signal processing on graphs strives to generalize definitions and operations from signal processing to data represented by a graph. An important definition in this field is the graph shift operator. In this paper we show that when defining the graph shift operator to be the Markov matrix, the framework of signal processing on graphs is strongly related to the diffusion map framework. We present and exemplify advantages that stem from this definition. In particular we present a computationally efficient solution to semi-supervised graph signal learning based on our suggested definition for the graph shift operator. We also suggest an alternative definition of signals defined over graphs, which relates the relationship between the signal and the underlying graph geometry.

APPENDIX

In this appendix, we prove Lemma 1 and Proposition 1.

A. Proof of Lemma 1

The normalized graph Laplacian is defined as

$$\mathbf{L} = \mathbf{D}^{-\frac{1}{2}} (\mathbf{D} - \mathbf{W}) \mathbf{D}^{-\frac{1}{2}} = \mathbf{I}_{N} - \mathbf{D}^{-\frac{1}{2}} \mathbf{W} \mathbf{D}^{-\frac{1}{2}}, \quad (60)$$

²https://github.com/mpf/spgl1.

and the Markov matrix is defined as

$$\mathbf{P} = \mathbf{D}^{-1}\mathbf{W} = \mathbf{D}^{-\frac{1}{2}} \left(\mathbf{D}^{-\frac{1}{2}} \mathbf{W} \mathbf{D}^{-\frac{1}{2}} \right) \mathbf{D}^{\frac{1}{2}}.$$
 (61)

It follows from (60) and (61) that

$$\mathbf{P} = \mathbf{D}^{-\frac{1}{2}} \left(\mathbf{I}_N - \mathbf{L} \right) \mathbf{D}^{\frac{1}{2}}. \tag{62}$$

This means that the Markov matrix is similar to $I_N - L$. The normalized graph Laplacian is a symmetric matrix and is thus diagonalizable. The same is true for $I_N - L$. As P is similar to a diagonalizable matrix, it is also diagonalizable.

B. Proof of Proposition 1 part 1

In the proof of Lemma 1 we saw that P is similar to $I_N - L$. It follows that L is similar to I - P,

$$\mathbf{I}_N - \mathbf{P} = \mathbf{D}^{-\frac{1}{2}} \mathbf{L} \mathbf{D}^{\frac{1}{2}}, \tag{63}$$

and that

$$(\mathbf{I}_N - \mathbf{P}) \mathbf{D}^{-\frac{1}{2}} = \mathbf{D}^{-\frac{1}{2}} \mathbf{L}. \tag{64}$$

It follows that

$$(\mathbf{I}_N - \mathbf{P}) \mathbf{D}^{-\frac{1}{2}} \mathbf{u}_i = \tilde{\lambda}_i \mathbf{D}^{-\frac{1}{2}} \mathbf{u}_i.$$
 (65)

Thus, $\mathbf{D}^{-\frac{1}{2}}\mathbf{u}_i$ is an eigenvector of $\mathbf{I}_N - \mathbf{P}$, with eigenvalue $\tilde{\lambda}_i$. Also,

$$(\mathbf{I}_N - \mathbf{P}) \mathbf{D}^{-\frac{1}{2}} \mathbf{u}_i = \mathbf{D}^{-\frac{1}{2}} \mathbf{u} - \mathbf{P} \mathbf{D}^{-\frac{1}{2}} \mathbf{u}_i = \tilde{\lambda}_i \mathbf{D}^{-\frac{1}{2}} \mathbf{u}_i,$$
 (66)

so that

$$\mathbf{P}\mathbf{D}^{-\frac{1}{2}}\mathbf{u}_{i} = \left(1 - \tilde{\lambda}_{i}\right)\mathbf{D}^{-\frac{1}{2}}\mathbf{u}_{i}.\tag{67}$$

This proves that if \mathbf{u}_i is an eigenvector of \mathbf{L} with eigenvalue $\tilde{\lambda}_i$, then $\mathbf{D}^{-\frac{1}{2}}\mathbf{u}_i$ is an eigenvector of \mathbf{P} with eigenvalue $1-\tilde{\lambda}_i$.

C. Proof of Proposition 1 part 2

We know from Proposition 1 part 1 that

$$\lambda_i = 1 - \tilde{\lambda}_i. \tag{68}$$

Let $\tilde{\lambda}_1$ be the smallest valued eigenvalue of the normalized graph Laplacian. As the normalized graph Laplacian is a positive semi definite matrix it follows that $\tilde{\lambda}_1 \geq 0$ and thus $\lambda_1 \leq 1$, where λ_1 is the largest eigenvalue of the Markov matrix.

Let λ_N be the largest valued eigenvalue of the normalized graph Laplacian. Chung [8] used the rayleigh quotient to prove that $\lambda_N \leq 2$. Therefore, $\lambda_N \geq -1$, where λ_N is the smallest eigenvalues of the Markov matrix.

REFERENCES

- Y. Lecun, L. Bottou, Y. Bengio, and P. Haffner, "Gradient-based learning applied to document recognition," *Proceedings of the IEEE*, vol. 86, no. 11, pp. 2278–2324, November 1998.
- [2] P. Hoff, A. Raftery, and M. Handcock, "Latent space approaches to social network analysis," *Journal of the American Statistical Association*, vol. 97, no. 460, pp. 1090–1098, 2002.
- [3] D. I. Shuman, S. K. Narang, P. Frossard, A. Ortega, and P. Vandergheynst, "The emerging field of signal processing on graphs: Extending high-dimensional data analysis to networks and other irregular domains," *IEEE Signal Processing Magazine*, vol. 30, no. 3, pp. 83–98, May 2013.
- [4] A. Sandryhaila and J. M. F. Moura, "Discrete signal processing on graphs," *IEEE Transactions on Signal Processing*, vol. 61, no. 7, pp. 1644–1656, April 2013.
- [5] —, "Discrete signal processing on graphs: Frequency analysis," *IEEE Transactions on Signal Processing*, vol. 62, no. 12, pp. 3042–3054, June 2014.
- [6] S. Chen, R. Varma, A. Sandryhaila, and J. Kovacevic, "Discrete signal processing on graphs: Sampling theory," *IEEE Transactions on Signal Processing*, vol. 63, no. 24, pp. 6510–6523, December 2015.
- [7] X. Dong, D. Thanou, P. Frossard, and P. Vandergheynst, "Learning laplacian matrix in smooth graph signal representations," *IEEE Transactions on Signal Processing*, vol. 64, no. 23, pp. 6160–6173, December 2016.
- [8] F. Chung, Spectral Graph Theory, ser. CBMS Regional Conference Series in Mathematics. American Mathematical Society, Providence, R.I., 1997, no. 92.
- [9] A. Sandryhaila and J. M. F. Moura, "Big data analysis with signal processing on graphs: Representation and processing of massive data sets with irregular structure," *IEEE Signal Processing Magazine*, vol. 31, no. 5, pp. 80–90, September 2014.
- [10] D. Zhou and B. Schölkopf, "A regularization framework for learning from graph data," in *ICML Workshop on Statistical Relational Learning*, 2004, pp. 132–127.
- [11] R. R. Coifman and S. Lafon, "Diffusion maps," Applied and Computational Harmonic Analysiss: Special issue on Diffusion Maps and Wavelets, vol. 21, pp. 5–30, July 2006.
- [12] Y. Keller and Y. Gur, "A diffusion approach to network localization," *IEEE Transactions on Signal Processing*, vol. 59, no. 6, pp. 2642 –2654, June 2011.
- [13] G. David, A. Averbuch, and R. R. Coifman, "Hierarchical clustering via localized diffusion folders," in *Manifold Learning and Its Applications, Papers from the 2010 AAAI Fall Symposium*, November 2010.
- [14] R. Talmon, I. Cohen, S. Gannot, and R. R. Coifman, "Diffusion maps for signal processing: A deeper look at manifold-learning techniques based on kernels and graphs," *IEEE Signal Process*ing Magazine, vol. 30, no. 4, pp. 75–86, July 2013.
- [15] Y. Keller, R. R. Coifman, S. Lafon, and S. W. Zucker, "Audiovisual group recognition using diffusion maps," *IEEE Transactions on Signal Processing*, vol. 58, no. 1, pp. 403–413, January 2010.
- [16] D. Zelazo and M. Bürger, "On the definiteness of the weighted laplacian and its connection to effective resistance," in 53rd IEEE Conference on Decision and Control, December 2014, pp. 2895–2900.
- [17] C. Fowlkes, S. Belongie, F. Chung, and J. Malik, "Spectral grouping using the Nyström method," *IEEE Transactions on Pattern Analysis and Machine Intelligence*, vol. 26, no. 214-225, pp. 1–52, January 2004.
- [18] E. J. Nyström, "Über die praktische auflösung von linearen integralgleichungen mit anwendungen auf randwewtaufgaben

- der potentialtheorie," Commentationes Physico-Mathematicae, vol. 4, no. 15, pp. 1–52, 1928.
- [19] C. T. H. Baker, *The Numerical Treatment of Integral Equations*. Oxford: Clarendon Press, 1977.
- [20] W. H. Press, S. Teukolsky, W. T. Vetterling, and B. P. Flannery, *Numerical Recipies in C*, 2nd ed. Cambridge University Press, 1992.
- [21] E. van den Berg and M. P. Friedlander, "Probing the pareto frontier for basis pursuit solutions," *SIAM J. on Scientific Computing*, vol. 31, no. 2, pp. 890 912, November 2008.
- [22] ——, "Sparse optimization with least-squares constraints," Univ of British Columbia, Tech. Rep., January 2010.